Journal of Inflammation Research

Dovepress
Taylor & Francis Group

Open Access Full Text Article

ORIGINAL RESEARCH

Low-Intensity Pulsed Ultrasound Promotes a Treg-Like Phenotype and Suppresses a Th17-Like Phenotype in CD4$^+$ T Cells via YAP/TAZ Activation in vitro

Renli Yang[1], Xirui Zhang[2], Yanjun Zhang[3], Yi Man[2], Xingmei Yang[2]

[1]State Key Laboratory of Oral Diseases & National Center for Stomatology & National Clinical Research Center for Oral Diseases & Department of Jinjiang Clinic, West China Hospital of Stomatology, Sichuan University, Chengdu, Sichuan, 610041, People's Republic of China; [2]State Key Laboratory of Oral Diseases & National Center for Stomatology & National Clinical Research Center for Oral Diseases & Department of Implantology, West China Hospital of Stomatology, Sichuan University, Chengdu, Sichuan, 610041, People's Republic of China; [3]Department of Stomatology, West China Xiamen Hospital of Sichuan University, Xiamen, Fujian, People's Republic of China

Correspondence: Xingmei Yang, State Key Laboratory of Oral Diseases & National Center for Stomatology & National Clinical Research Center for Oral Diseases & Department of Implantology, West China Hospital of Stomatology, Sichuan University, Chengdu, Sichuan, 610041, People's Republic of China, Tel +86-28-85503571, Email yangxingmei_scu@scu.edu.cn

Introduction: CD4$^+$ T cell subpopulations, particularly T helper 17 (Th17) and regulatory T (Treg) cells, exhibit antagonistic functions and play essential roles in inflammatory responses. Yes-associated protein (YAP) and transcriptional coactivator with PDZ-binding motif (TAZ) are critical modulators of cell proliferation and differentiation. Low-intensity pulsed ultrasound (LIPUS) has been shown to regulate YAP/TAZ activity, but its role in Th17/Treg balance remains unclear.

Methods: CD4$^+$ T cells were purified from rat peripheral blood mononuclear cells (PBMCs) using magnetic-activated cell sorting (MACS). The cells were then treated with low-intensity pulsed ultrasound (LIPUS) at a set of parameters (1.0 MHz, 20 mW/cm², 20% duty cycle, 2h/day for 3 days) optimized based on preliminary proliferation and apoptosis assays. The effects of LIPUS on the expression of key functional markers (Foxp3 for Treg-like cells and IL-17A for Th17-like cells) were evaluated by flow cytometry, quantitative PCR, and ELISA. The activation and subcellular localization of YAP/TAZ were examined using immunofluorescence staining. Furthermore, siRNA-mediated knockdown was performed to investigate the functional involvement of YAP/TAZ in the LIPUS-mediated effects.

Results: LIPUS treatment significantly increased the frequency of Foxp3-expressing cells while decreasing the frequency of IL-17A-producing cells. Additionally, LIPUS promoted the activation and nuclear translocation of YAP and TAZ, as evidenced by enhanced protein expression and a shift in subcellular localization. siRNA-mediated knockdown of YAP/TAZ attenuated the LIPUS-induced increase in Foxp3$^+$ cells and potentiated the population of IL-17A$^+$ cells. Importantly, LIPUS treatment effectively rescued the expression patterns of these functional markers following YAP/TAZ inhibition.

Discussion: Our findings demonstrate that LIPUS promotes a Treg-like phenotype and suppresses a Th17-like phenotype in CD4$^+$ T cells, a process that is mediated, at least in part, by the activation of the YAP/TAZ signaling pathway. This immunomodulatory effect suggests that LIPUS could be explored as a novel non-invasive strategy for managing autoimmune diseases and chronic inflammatory conditions associated with an imbalance in T cell responses.

Keywords: low-intensity pulsed ultrasound, Treg, Th17, YAP, TAZ

Introduction

Chronic inflammation jeopardizes the prognosis of bone reconstruction in many scenarios, such as fracture healing, rheumatoid arthritis, tumors, pre-eclampsia, atherosclerosis, autoimmune hepatitis, periodontitis, ulcerative colitis, and so on.[1–3]T cells play diverse roles in the immune response and are germane to the modulation of inflammation. Various CD4$^+$T cells, especially the regulatory T(Treg) and T helper 17(Th17) subsets have emerged as pivotal players across

Received: 19 June 2025
Accepted: 26 September 2025
Published: 2 October 2025

a variety of diseases involving inflammation.[4,5] Th17 and Treg cells are functionally antagonistic subsets of $CD4^+$T cells, which is the hard core of adaptive immunity.[4] Th17 can cause severe inflammatory diseases in humans, resulting in chronic inflammation, autoimmune disorders, cancer, and bone loss. However, the pathogenicity can be limited by Treg, which serves as a vital mechanism of negative regulation of immune activities to establish self-tolerance and prevent autoimmunity and maintain homeostasis.[6–11] Generally, the Th17 and Treg cell subsets are in a state of equilibrium to reach host immune homeostasis; however, an imbalance of Th17/Treg will lead to various autoimmune diseases and inflammation. Th17 cells are characterized by secretion of IL-17A, and expression of transcriptional factor retinoid-related orphan nuclear receptor (ROR)γt, which induces transcription of *Il17A*, and is regulated by multiple cytokines; IL-6, IL-1β, IL-23, and transforming growth factor (TGF)-β are known to drive Th17 differentiation.[12–14] Treg cells, accomplishing differentiation in either thymus (tTreg) or periphery (pTreg), are characterized by expression of transcriptional factor forkhead box P3 (Foxp3) and persistent expression of the surface markers CD25 and cytotoxic T lymphocyte-associated molecule-4 (CTLA-4).[15] T cell receptor (TCR) signaling plays a pivotal role in Treg differentiation from naïve $CD4^+$T cells, whereas TGF-β, thrombospondin-1 (TSP-1), and retinoic acid (RA) are also reported to signal $CD4^+$T cells to differentiate to Treg.[16–18]

Researchers recently found that two key effectors of the Hippo signaling pathway, YAP, and TAZ, also participated in regulating the Treg/Th17 differentiation and played pivotal roles.[19,20] YAP has been known as the main player in the Hippo signaling pathway, participating in the regulation of organ size and maintaining the dynamic balance of cell proliferation and apoptosis. Research shows that YAP can promote the tumor inhibition function of Treg cells, enhance the expression of Foxp3, and enhance the function of Treg when YAP protein is dephosphorylated and activated; on the contrary, the lack of YAP will lead to the dysfunction of Treg, failing to activate the immunosuppressant function of Treg cells in autoimmune diseases.[19] Vimal et al demonstrate that YAP/TAZ function within epicardial derivatives to drive the production of the Treg inducer, interferon (IFN)-γ; after myocardial injury, YAP/TAZ mutant mice exhibit a significant deficiency of Tregs in the injured myocardium, causing severe myocardial fibrosis and increased mortality.[20]

Cell behavior can be fundamentally affected by physical and mechanical contact between cells and their extracellular matrix (ECM). Mechanical stimulation can improve tissue regeneration in a host of cell types, including mesenchymal stem cells, osteoblasts, chondrocytes, epithelial cells, and muscle cells.[21] Besides, recent researches suggest that YAP and TAZ are responsible for sensing and transducing mechanical cues, from shear stress, and cell shape to extracellular matrix rigidity, and translating them into cell-specific transcriptional programs.[22] YAP and TAZ serve as sensors and mediators of mechanical signals exerted by mechanical cues through integrin-dependent focal adhesions (FA) formation linking with Rho GTPase activity and tension of the actomyosin cytoskeleton, instead of the Hippo/LATS cascade.[23,24] In this case, it is logical to speculate that YAP/TAZ will react to artificially applied mechanical cues. The fact is that low-intensity pulsed ultrasound (LIPUS), as a non-invasive treatment method, can accelerate bone fracture healing by activating YAP/TAZ.[25] LIPUS is capable of delivering ultrasound at a low intensity and outputting in the mode of pulsed waves, thus transforming sound energy to mechanical energy, which shows promising prospects in the treatment or remission of various diseases, such as fracture healing, neuromodulation, soft-tissue regeneration and inhibition of inflammation.[26–30] Besides, our previous study has proved that LIPUS can promote osteogenic differentiation of mesenchymal stem cells.[31] Although the various impacts of LIPUS have been discussed so far, which has even been approved by FDA as a therapy for bone fracture, the anti-inflammatory properties remain the jewel of these functions. However, few studies have focused on the effects of LIPUS on Treg/Th17 differentiation, which will hinder the full understanding of the mechanism by which LIPUS exerts its therapeutic effects. The vast gap in this area needs to be filled.

This study investigates the immunomodulatory effects of low-intensity pulsed ultrasound (LIPUS) on CD4+ T cell function, using an experimental approach outlined in Figure 1. We specially focus on markers associated with regulatory and pro-inflammatory T cell responses. Through a series of in vitro experiments, we examine how LIPUS influences the expression of key functional markers such as Foxp3 and IL-17A, and explore the involvement of YAP and TAZ signaling in this process. This research provides foundational insights into the mechanobiological regulation of immune cell function, establishing a basis for further exploration in this field.

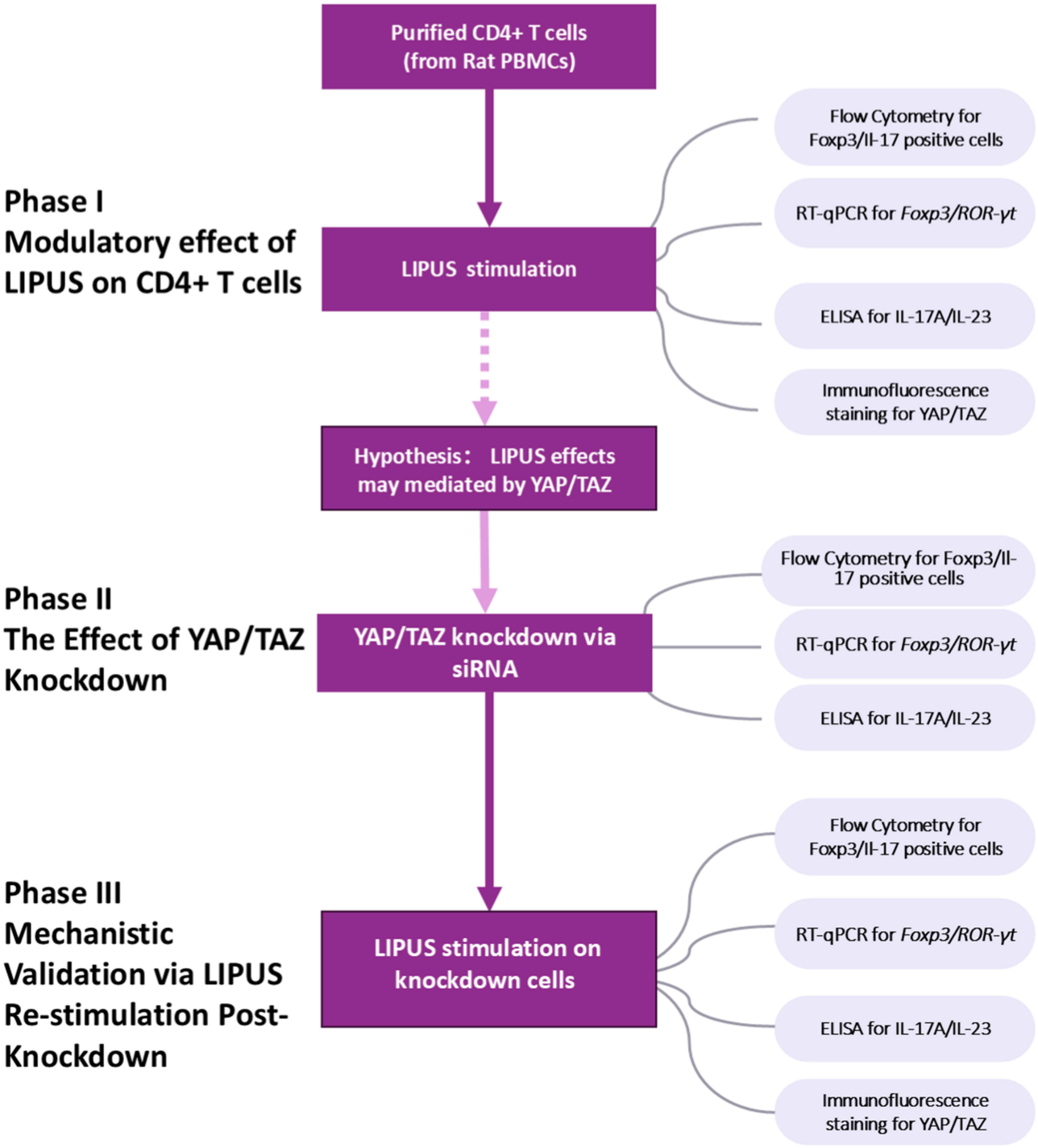

Figure 1 Schematic diagram depicting the experimental design. Three sequential experimental phases are shown: initial LIPUS stimulation and functional characterization; genetic inhibition of YAP/TAZ expression using siRNA-mediated knockdown; and final mechanistic validation through LIPUS re-stimulation of knockdown cells.

Materials and Methods

Cell Preparation, Culture, and Sorting

All animal experiments described in this report were approved by the Sichuan University Animal Care and Use Committee. In total, 50 Sprague-Dawley rats were used. The ethics committee number of this experiment is WCHSIRB-D-2020043. All animal experiments complied with the ARRIVE guidelines and were carried out in accordance with the UK Animals (Scientific Procedures) Act, 1986 and associated guidelines, EU Directive 2010/63/

EU for animal experiments. We ensured humane endpoints, minimized animal numbers, and provided appropriate housing (eg, SPF conditions) and analgesia protocols.

10mL blood was extracted from the aorta of SD rats, transferred into a 50mL centrifuge tube, diluted with 10mL PBS solution, and gently mixed. Prepare two 15mL centrifuge tubes, and add 5mL Ficoll solution (Sigma-Aldrich, MO, USA) into each tube, then gently add 10mL diluted blood to each tube to avoid mixing two solutions. Centrifuge at 2,000rpm for 20 min. The cell layer is white, and the cells are transferred into another 15mL centrifuge tube using an Eppendorf pipette. Add 10–15mL PBS solution to resuspend, and the centrifuge at 1,500rpm for 10min. Remove the supernatant, add DMEM medium (Gibco by Invitrogen, CA, USA), and centrifuge. Resuspend the cells with a 5–10mL medium with 10% fetal bovine serum (FBS, Gibco) and transfer the cell suspension into a T25 cell culture flask (Corning, NY, USA).

Rat PBMC obtained by the above method were cultured in DMEM (containing 10% FBS) in a CO_2 incubator (Thermo, USA) at 37 °C, 5% CO_2, and 90% relative humidity. Cell growth was observed daily using an inverted microscope (OLYMPUS CX23, Japan). When dense monolayer cells were formed, the cells were treated with 3–5mL 0.25% Trypsin-EDTA (Gibco) at 37 °C for 3~5 min. DMEM medium containing 10% FBS was added to terminate digestion. The cell suspension was transferred to a 15mL centrifuge tube for centrifugation at 1500rpm for 3min. 10mL DMEM medium (containing 10% FBS) was added to resuspend the cells and evenly transferred to two T25 flasks. All cells were used for experiments before passage 10.

$CD4^+$T cells were sorted from PBMC by magnetic-activated cell sorting (MACS). Rat CD4 monoclonal antibody (MA5-17387) was purchased from Invitrogen. The purity of purified $CD4^+$T cells was identified by cell flowmetry and showed in Supplementary Figure 1, which was 96.59±0.79%. The $CD4^+$T cells were resuspended in RPMI (Gibco) containing 10% FBS and cultured in a T25 cell culture flask in a CO_2 incubator at 37 °C, 5% CO_2, and 90% relative humidity for six hours.

Low-Intensity Pulsed Ultrasound (LIPUS) Exposure

The LIPUS device, its signal, and how it acted on cells were described in our previous studies.[21] Based on literature and our previous work, 1.0 MHz frequency, 20% duty cycle, and 20 mW/cm^2 intensity of LIPUS for cells is reasonable and do not cause heat damage or proliferation.[21] Cells to be treated by LIPUS were seeded in the central 3 wells in 12-well plates. The LIPUS device consisted of an array of three transducers, each 20 mm in diameter. The plates were placed on the ultrasound transducer array conducted by a thin layer of coupling gel. All LIPUS treatments were performed in the tissue culture incubator (37 °C, 5% CO_2, 95% humidity). Controls were prepared in the same way without switching on the machine.

Cell Viability

Cell viability was quantitatively assessed using two complementary methods: (1) metabolic activity via Cell Counting Kit-8 (CCK-8; Dojindo Molecular Technologies, Inc., Kumamoto, Japan) and (2) ATP content via CellTiter-Glo Luminescent Cell Viability Assay (Promega Corporation, Madison, WI, USA) measuring luminescent signal generated by luciferase-catalyzed ATP hydrolysis. Both assays were performed according to manufacturers' protocols with three technical replicates per condition, using cell-free medium as blank controls. The $CD4^+$T cells were seeded with a density of 10^5/well in 12-well plates and then treated with LIPUS (1.0 MHz and 20 mW/cm^2 at 20% duty cycle) continuously for 0, 0.5, 2, 6, 12, and 24h per day. Then the following operations were carried out respectively.

(a) After three days, 20μL CCK-8 solution was added to each well, and the cells were incubated at 37 °C for 4 h. After incubation, absorbance at 450 nm was measured using an *EPOCH2* microplate reader (BioTek Instruments, Inc., Winooski, VT, USA) to assess cell viability.

(b) After three days, 100μL CTG solution was added to each well, and the plates were kept at room temperature for 10min. Luminescence was measured for each well using a microplate reader (BioTek). All luminescence readings in the CTG assay were normalized to blank wells (containing medium alone without cells) to account for background signals.

YAP and TAZ Silencing

Gene silencing of YAP and TAZ was achieved using ON-TARGETplus SMARTpool siRNA reagents (Thermo Fisher Scientific, Waltham, MA, USA) containing four optimized siRNA sequences per target (Table 1). $CD4^+$ T cells were transfected with 50 nM siRNA using Lipofectamine™ 2000 Transfection Reagent (Thermo Fisher Scientific) at a 1:1

Table 1 Nucleotide Primers Used for Quantitative Polymerase Chain Reaction and siRNA Sequence

Genes	Oligonucleotide Sequence
RORγt	Forward: GATGCAGTTAATGCCCCACT Reverse: TTCCTTATTGGGGTCAGCAC
Foxp3	Forward: AGGTATCCATCCATCCCACA Reverse: TGCCACAGTTCTCAAAGCAC
YAP	Forward: CCAGACGACTTCCTGAACAGCG Reverse: GCATCTCCTTCCAGTGTGCCAA
TAZ	Forward: TCTTATCACCGTCTCTAACCAC Reverse: CCTTGGTGAAGCAGATGTCTGC
GAPDH	Forward: GCCCAGCAAGGATACTGAGA Reverse: GGTATTCGAGAGAAGGGAGGGC
YAP siRNA	GCAUCUUCGACAGUCUUCUTT
TAZ siRNA	GCCACAUCUGAACCUGAAGUUGAU

(μL: μg) ratio in Opti-MEM™ Reduced Serum Medium (Thermo Fisher Scientific). Following 6-hour incubation at 37 °C/5% CO_2, the transfection mixture was replaced with complete RPMI-1640 medium (Gibco) containing 10% FBS. Knockdown efficiency (>70%) was verified at both mRNA (by qPCR) and protein (by Western blot) levels 48 hours post-transfection, using GAPDH as loading control. Non-targeting siRNA (Thermo Fisher Scientific) and mock transfection controls were included in all experiments.

Elisa

Serum concentrations of IL-17A, IL-23, and IL-10 were quantified using commercial ELISA kits (Rat IL-17, IL-23, and IL-10 Elisa kits; Shanghai Jianglai Biotechnology Co., Ltd., Shanghai, China) according to the manufacturer's protocols. Briefly, 100 μL of standards or 1:4 diluted serum samples were added to pre-coated 96-well plates in duplicate and incubated for 90 min at 37 °C. After washing five times with 300 μL wash buffer, 100 μL biotinylated detection antibody was added and incubated for 1 h at 37 °C. Following another wash cycle, 100 μL streptavidin-HRP was added for 30 min at 37 °C protected from light. After final washing, 90 μL TMB substrate was added for 15 min at room temperature, and the reaction was stopped with 50 μL stop solution. Absorbance was immediately measured at 450 nm with wavelength correction at 570 nm using a SpectraMax i3x microplate reader (Molecular Devices, San Jose, CA, USA). Sample concentrations were calculated from standard curves ($r^2 > 0.99$ for all assays) using SoftMax Pro 7.0 software (Molecular Devices).

RNA Isolation and RT-qPCR

Total RNA was extracted from trypsinized cells (0.25% trypsin-EDTA; Thermo Fisher Scientific, Waltham, MA, USA) using 1 mL TRIzol™ Reagent (TIANGEN Biotech, Beijing, China) according to the manufacturer's protocol. RNA quality was verified by electrophoresis (28S:18S rRNA ratio >1.8) and quantified by NanoDrop spectrophotometry (A260/280 ratio 1.9–2.1). Reverse transcription was performed with 1 μg total RNA using the PrimeScript™ mRNA Selective PCR Kit (Takara Bio Inc., Kusatsu, Shiga, Japan) in 20 μL reactions with oligo(dT) primers. Quantitative PCR was conducted in triplicate 10 μL reactions containing 1 μL cDNA template, 200 nM gene-specific primers (Table 1), and PowerUp™ SYBR™ Green Master Mix (Thermo Fisher Scientific) on a StepOnePlus™ Real-Time PCR System (Applied Biosystems, Foster City, CA, USA) under standardized conditions: 95 °C for 2 min, followed by 40 cycles of 95 °C for 15 sec and 60 °C for 1 min, with melt curve analysis (60–95 °C, 0.3 °C/sec increment). Gene expression was normalized to GAPDH and calculated using the $2^{(-\Delta\Delta Ct)}$ method, with amplification efficiencies (90–110%) validated by standard curve analysis.

Immunofluorescence Staining

Cells cultured in 12-well plates were washed three times with PBS (pH 7.4) and fixed with 4% paraformaldehyde (Electron Microscopy Sciences, Hatfield, PA, USA) in PBS for 15 min at room temperature. After PBS washing, cells were permeabilized with 0.5% Triton™ X-100 (Sigma-Aldrich, St. Louis, MO, USA) for 20 min, followed by blocking with 0.5% bovine serum albumin (BSA; Thermo Fisher Scientific, Waltham, MA, USA) in PBS for 30 min at room temperature. Cells were then incubated overnight at 4 °C with rabbit polyclonal anti-YAP antibody (1:100; Cell Signaling Technology, Danvers, MA, USA) and rabbit polyclonal anti-TAZ antibody (1:100; Santa Cruz Biotechnology, Dallas, TX, USA). After PBS washes, samples were incubated for 1 h at room temperature with Cy3-conjugated goat anti-rabbit IgG (H+L) (1:200; Beyotime Biotechnology, Shanghai, China) or Cy3-conjugated goat anti-mouse IgG (H+L) (1:200; Beyotime Biotechnology). Nuclei were counterstained with 1 μg/mL DAPI (Thermo Fisher Scientific) for 5 min at room temperature. Fluorescent images were acquired using an FV1000 laser scanning confocal microscope (Olympus Corporation, Tokyo, Japan) with a 60× oil immersion objective, collecting z-stack images at 0.5 μm intervals. To minimize photobleaching and ensure accurate fluorescence measurement, images were acquired under conditions optimized for exposure time and light intensity. Specifically, the exposure time was adjusted based on fluorescence intensity to avoid overexposure, and the laser power was reduced to limit potential photobleaching, while ensuring sufficient signal detection. Imaging was performed with consistent settings across all samples to maintain reliability. Fluorescent images were processed using FV10-ASW software (v4.2). To quantify the relative fluorescence intensity, three independent experiments were performed. For each experiment, one image was captured at 200× magnification. Fluorescence intensity was measured using ImageJ software (National Institutes of Health), normalized to the control group, and statistically analyzed in GraphPad Prism 8.0 (GraphPad Software, San Diego, CA, USA).

Flow Cytometry

Harvested cells were trypsinized, collected, and quantified using a hemocytometer, then diluted in PBS to 1×10^6 cells/mL. After centrifugation of 200 μL aliquots (1000 × g, 5 min, 4 °C), cell pellets were washed twice with 1 mL ice-cold PBS and resuspended in 100 μL PBS. For immunophenotyping, three technical replicates per group (n = 3) were prepared with the following antibody combinations: (1) Negative control: 100 μL unstained cell suspension; (2) $CD4^+$ T-cell purity: 100 μL suspension + 0.5 μg FITC-conjugated anti-CD4 (Clone OKT4; Thermo Fisher Scientific, Waltham, MA, USA); (3) Intracellular markers: 100 μL suspension + 2 μL each of FITC-conjugated anti-Foxp3 (Clone 236A/E7; Thermo Fisher) and PerCP-Cy5.5-conjugated anti-IL-17A (Clone eBio64DEC17; Thermo Fisher). For the intracellular staining of Foxp3 and IL-17A, cells were first fixed and permeabilized using the Foxp3/Transcription Factor Staining Buffer Set (eBioscience™, Thermo Fisher Scientific) according to the manufacturer's instructions, prior to antibody incubation. All tubes were incubated for 1 h at 4 °C protected from light, followed by centrifugation (3000 × g, 10 min) and two washes with 400 μL PBS. Samples were acquired immediately on a NovoCyte 3000 flow cytometer (ACEA Biosciences Inc., San Diego, CA, USA) with ≥50,000 events recorded per sample. Data were analyzed using FlowJo software (v10.8; BD Life Sciences, Franklin Lakes, NJ, USA) and FCS Express (v7; De Novo Software, Glendale, CA, USA). The gating strategy was applied as follows: cells were first gated on a forward scatter (FSC-A) vs side scatter (SSC-A) plot to identify the live lymphocyte population. Singlets were then selected using FSC-H vs FSC-A to exclude doublets. $CD4^+$ T cells were identified from the singlet gate. Subsequent analysis for Foxp3 and IL-17A expression was performed on the $CD4^+$ population, with positive gates rigorously set based on fluorescence-minus-one (FMO) controls. A detailed graphical representation of the gating strategy is provided in Supplementary Figure 2.

Statistical Analysis

Data are presented as mean values ± standard error of the mean. Statistical computation was performed in GraphPad Prism 8.0 (GraphPad Software, San Diego, CA, USA), and statistical significance was analyzed using one-way ANOVA analysis followed by Tukey's multiple comparison tests. Unless otherwise noted, $p<0.05$ was considered statistically significant.

Results

LIPUS Promotes a Treg-Like Phenotype in CD4$^+$T Cells

Rat CD4$^+$ T cells were purified from PBMCs using MACS, as described in the Methods. To determine the optimal LIPUS exposure duration for CD4$^+$ T cell proliferation, we performed preliminary CCK-8 and CTG assays on cells treated for 0, 0.5, 2, 6, 12, and 24 hours per day for three days. These analyses revealed that 2 hours per day (2h/d) of LIPUS exposure significantly enhanced proliferation compared to other durations (Supplementary Figure 3). Consequently, 2h/d was selected for all subsequent experiments.

Cells were divided into two groups: the "LIPUS" group received daily 2h LIPUS treatment, while the "Ctrl" group were prepared in the same way without switching on the machine. Cells were harvested after three days. Initially, a series of experiments were conducted to assess whether the optimized LIPUS regimen (1.0 MHz, 20 mW/cm², 20% duty cycle, 2h/d) would induce significant apoptosis or attenuate cell proliferation. The results indicated that LIPUS exposure not only maintained cell viability (Figure 2a), but also significantly enhanced metabolic activity (CCK-8 assay) and ATP production (CTG assay) in CD4$^+$ T cells (Figure 2b). We next investigated the modulatory effect of LIPUS on CD4$^+$T cell functional marker expression. Flow cytometric analysis revealed that LIPUS treatment significantly increased the frequency of Foxp3-positive cells while decreasing the frequency of IL-17A-positive cells compared to the Ctrl group (Figure 3a). At the transcriptional level, qPCR analysis indicated that LIPUS significantly upregulated *Foxp3* mRNA expression while downregulating *RORγt* mRNA expression (Figure 3b). Furthermore, cytokine profiling via ELISA showed that LIPUS markedly suppressed the secretion of IL-17A and IL-23 (Figure 3c). These coordinated changes at the protein, transcriptional, and secretory levels consistently indicate that LIPUS promotes a Treg-associated functional characteristics while suppressing Th17-associated responses.

LIPUS Enhances YAP/TAZ Protein Levels in CD4$^+$ T Cells

As key regulators of cell proliferation, apoptosis, and mechanotransduction, YAP and TAZ are critical for cellular responses to mechanical stimuli. To determine whether LIPUS affects their expression and activation, CD4$^+$ T cells were divided into two groups: the LIPUS group received daily 2-hour stimulation for three days, while the Ctrl group prepared in the same way without switching on the machine.

Immunofluorescence analysis revealed that LIPUS treatment significantly enhanced the fluorescence signal of both YAP and TAZ, suggesting an overall increase in their protein expression levels (Figure 4a and b). Qualitative observation of the images suggested a potential shift in the subcellular localization of both proteins towards the nucleus following LIPUS stimulation. However, as our quantitative analysis was based on total fluorescence intensity, the primary supported conclusion is that of a global increase in YAP/TAZ protein levels.

YAP/TAZ Knockdown Modulates the Expression of Treg/Th17-Associated Markers

To investigate the involvement of YAP and TAZ in the regulation of Treg/Th17-associated markers, we inhibited their expression in CD4$^+$ T cells using siRNA. Cells were transfected with YAP-targeting siRNA (iYAP group), TAZ-targeting siRNA (iTAZ group), or a non-targeting scrambled siRNA (Ctrl group) for subsequent analysis.

RT-qPCR confirmed successful knockdown, showing significantly reduced *Yap* and *Taz* mRNA levels in the iYAP and iTAZ groups, respectively, compared to Ctrl (Figure 5a). Cell viability assessment (Supplementary Figure 4) revealed no significant differences between groups, indicating siRNA treatment did not affect cell activity. Flow cytometry analysis demonstrated that YAP or TAZ knockdown significantly decreased the frequency of Foxp3$^+$ cells while markedly increasing the frequency of IL-17A$^+$ cells compared to Ctrl (Figure 5b). No significant difference was observed between the iYAP and iTAZ groups. Consistent with these findings, RT-qPCR showed that knockdown of either YAP or TAZ significantly downregulated *Foxp3* mRNA expression and upregulated *RORγt* mRNA expression (Figure 5c). Similarly, ELISA detected significantly increased secretion of the Th17-associated cytokines IL-17A and IL-23 in both knockdown groups compared to Ctrl (Figure 5d). These results demonstrate that inhibition of either YAP or TAZ decreased Treg-related and increased Th17-related signatures. The nearly identical outcomes following YAP or TAZ knockdown suggest a functional redundancy between these transcriptional regulators in modulating this balance.

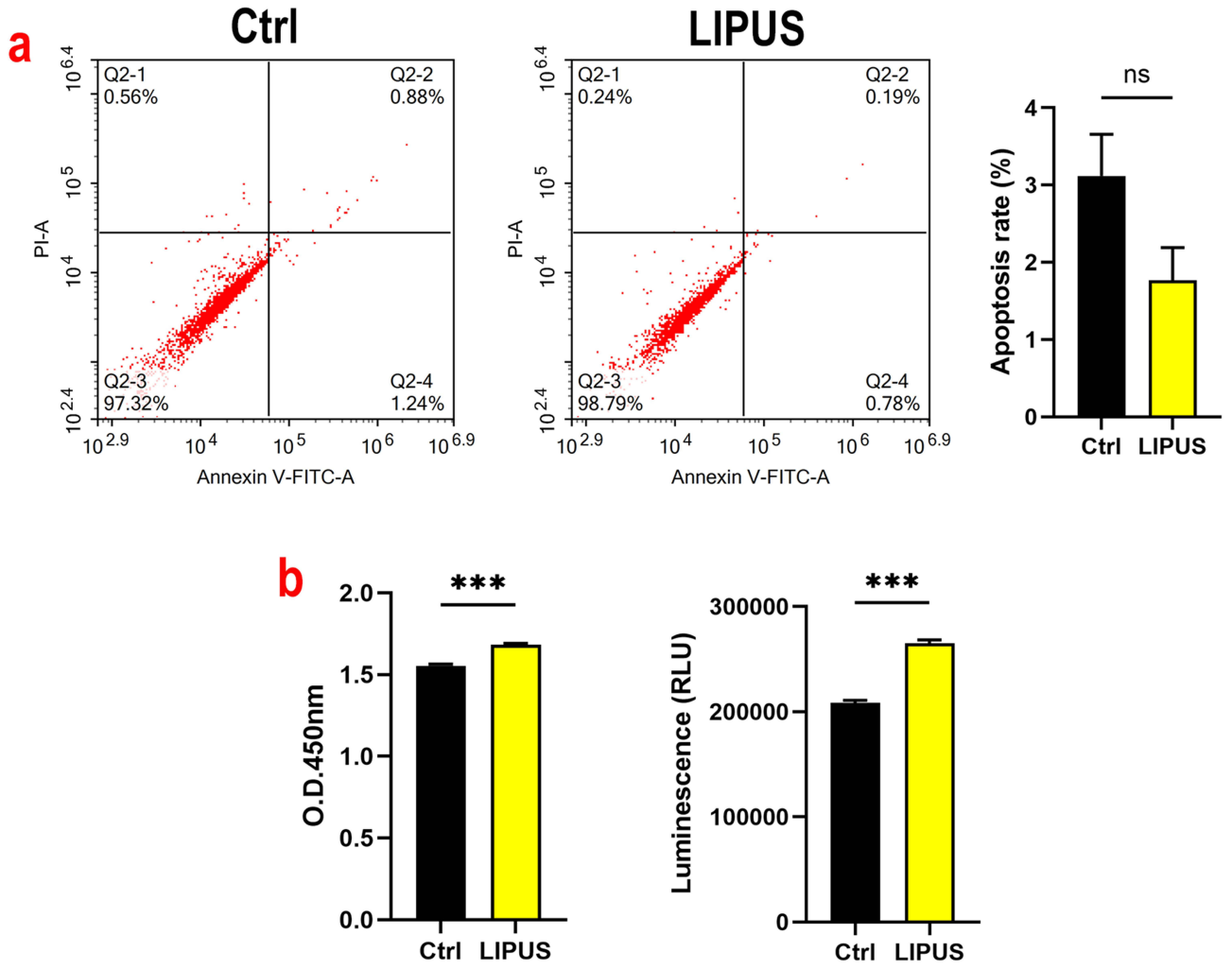

Figure 2 LIPUS exposure does not induce apoptosis but promotes viability and metabolic activity in $CD4^+$ T cells. Cells were treated with LIPUS (1.0 MHz frequency, 20% duty cycle, and 20 mW/cm^2 intensity) for 2 h/day over 72 hours (LIPUS group) versus untreated controls (Ctrl group). (**a**) Apoptotic rates were quantified by Annexin V-FITC/PI staining. (**b**) Cell viability was assessed using the CCK-8 assay(left); Cellular ATP levels were determined by the CellTiter-Glo (CTG) luminescent assay(right). Data represent mean ± SEM (n = 3 independent experiments). Statistical significance was determined by two-tailed Student's *t*-test (***p<0.001) versus the untreated control group, ns = not significant.

LIPUS Modulated Treg/Th17 Balance Through Regulation of YAP/TAZ Expression

Based on our findings linking YAP/TAZ to Treg/Th17 balance, we hypothesized that LIPUS modulates this balance through YAP/TAZ signaling. To test this, we applied LIPUS (2h/d for 3 days) to $CD4^+$ T cells with YAP or TAZ knockdown (iYAPL and iTAZL groups, respectively). Cells were then harvested for analysis.

Immunofluorescence analysis revealed that LIPUS treatment significantly increased the diminished YAP and TAZ fluorescence signals in siRNA-transfected cells (Figure 6a). Quantitative analysis of the relative MFI confirmed this mitigating effect in the respective knockdown groups (iYAPL and iTAZL) compared to their knockdown-only controls (iYAP and iTAZ) (Figure 6b). Furthermore, flow cytometry analysis revealed that LIPUS treatment significantly modulated the expression of key functional markers following YAP/TAZ knockdown. Compared to the knockdown-only groups (iYAP and iTAZ), the groups receiving combined knockdown and LIPUS treatment (iYAPL and iTAZL) exhibited a significant increase in the frequency of Foxp3-positive cells and a concurrent decrease in the frequency of IL-17A-positive cells (Figure 7a). Molecular analysis confirmed this restorative trend at the transcriptional and secretory levels: RT-qPCR showed LIPUS significantly elevated *Foxp3* mRNA and reduced *Il17a* mRNA in iYAPL/iTAZL cells compared to iYAP/iTAZ controls (Figure 7b). Similarly, ELISA detected significantly lower levels of the Th17-associated cytokines IL-17A and IL-23 in iYAPL/iTAZL groups versus iYAP/iTAZ groups (Figure 7c). Notably, Treg-

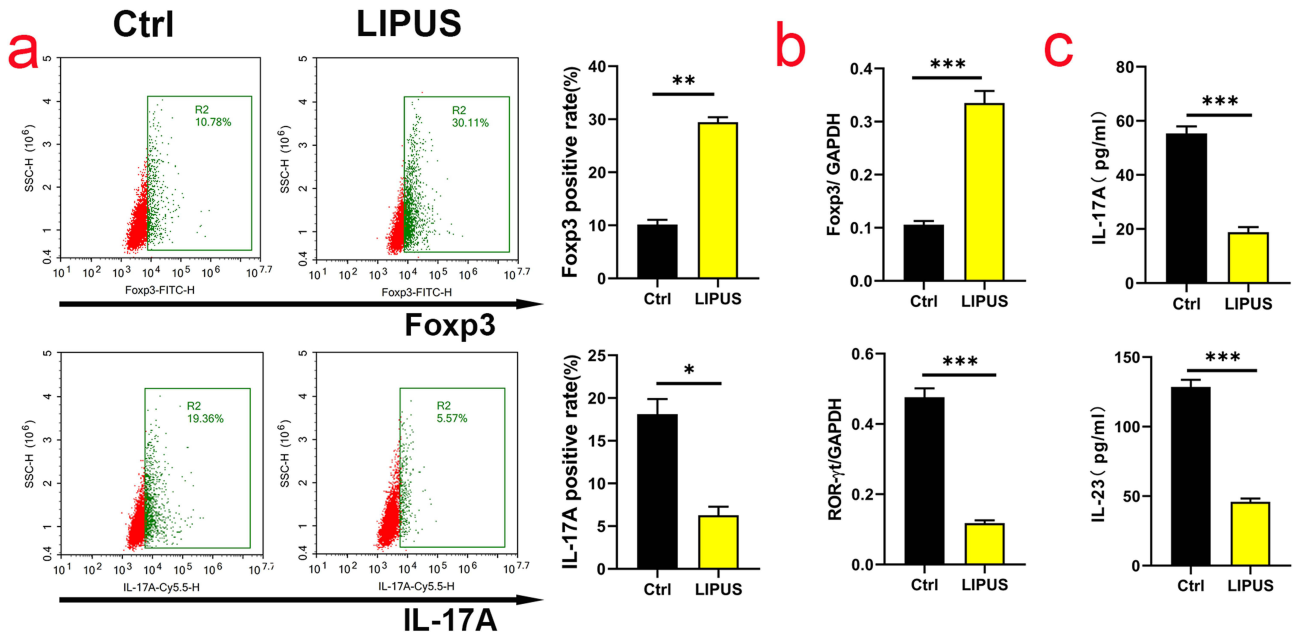

Figure 3 LIPUS promotes a Treg-like phenotype while suppresses a Th17-like phenotype in CD4$^+$ T cells. (**a**) Flow cytometry analysis of intracellular Foxp3 (a Treg marker) and IL-17A (a Th17 marker) expression in CD4$^+$ T cells following LIPUS treatment (1.0 MHz frequency, 20% duty cycle, and 20 mW/cm^2 intensity, 2 h/day for 3 days). Left: Representative flow plots. Right: Quantification of the frequencies of Foxp3$^+$ and IL-17A$^+$ cells. (**b**) qPCR quantification of *Foxp3* and *RORγt* mRNA levels normalized to *Gaphd*. (**c**) ELISA measurement of IL-17 and IL-23 cytokine secretion in culture supernatants. Data represent mean ± SEM from three independent experiments (n=3 biological replicates). Statistical significance was determined by two-tailed Student's *t*-test (*p<0.05, **p<0.01, ***p<0.001) versus the untreated control group.

associated markers in the iYAPL and iTAZL groups remained elevated compared to the LIPUS-only treated control cells. Collectively, these results demonstrate that the YAP/TAZ pathway is integral to the mechanism by which LIPUS modulates the expression of Treg- and Th17-associated markers.

Discussion

CD4$^+$ T cells differentiate into specialized subsets—including Th1, Th2, Th17, Treg, Th9, Th22, and T follicular helper (Tfh) cells—central to adaptive immunity. Among these, the balance between regulatory T (Treg) cells and T helper 17 (Th17) cells critically regulates immune homeostasis and prevents autoimmunity.[11,32] Disruption of this Treg/Th17 equilibrium is implicated in diverse pathologies, including cancer, rheumatoid arthritis (RA), systemic lupus erythematosus (SLE), pre-eclampsia (PE), atherosclerosis (AS), autoimmune hepatitis, periodontitis, and ulcerative colitis (UC).[1,11,33–38] Yes-associated protein (YAP) and transcriptional coactivator with PDZ-binding motif (TAZ), core effectors of the Hippo pathway, are now recognized as key mediators of cellular mechanotransduction.[22] Significantly, YAP/TAZ signaling directly influences Treg and Th17 differentiation.[19,20,39] Low-intensity pulsed ultrasound (LIPUS), which delivers mechanical energy via pulsed acoustic waves, is gaining attention as a promising approach for enhancing tissue regeneration in both experimental and clinical setting.[40,41] Our prior research demonstrated LIPUS's ability to regulate osteogenic differentiation in adipose-derived stem cells.[31] Given the diverse biological effects of low-intensity pulsed ultrasound (LIPUS) reported previously, we investigated its unexplored role in regulating Treg and Th17 cell differentiation. CD4$^+$ T cells were isolated from Sprague-Dawley rats for this study, as murine aortic blood collection presents significant technical challenges and yields limited cell numbers. Peripheral blood mononuclear cells (PBMCs) were purified from rat blood, and CD4$^+$ T cells were subsequently isolated using magnetic-activated cell sorting (MACS). Based on preliminary proliferation assays (Supplementary Figure 3), we optimized the LIPUS exposure duration (2h/day) for all subsequent experiments.

First, we confirmed that LIPUS treatment did not affect CD4$^+$ T cell viability (Figure 2). Flow cytometry analysis revealed that LIPUS significantly increased the frequency of Foxp3 positive cells while decreasing the frequency of IL-17A positive cells (Figure 3a). This shift in cell markers was further supported by elevated *Foxp3* mRNA expression and

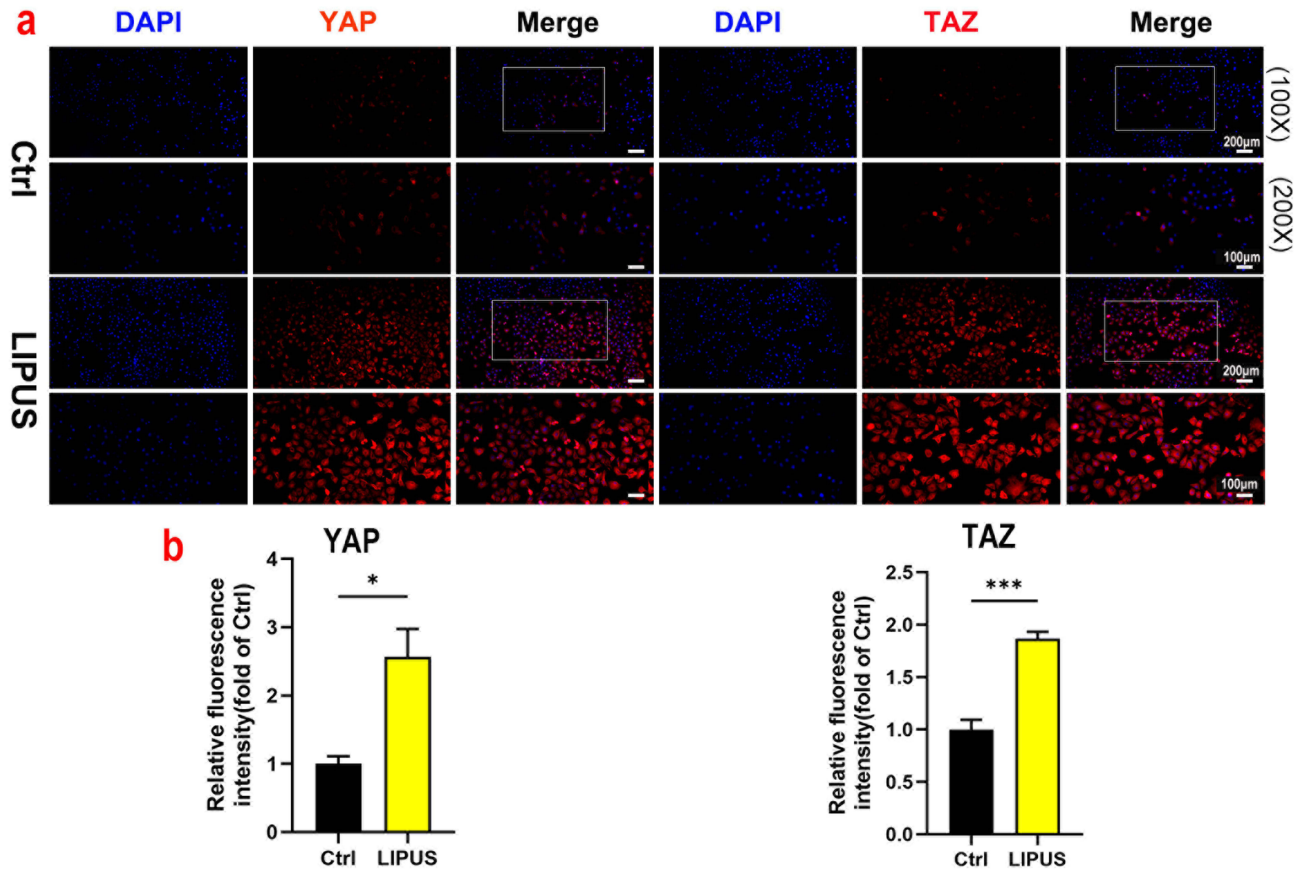

Figure 4 LIPUS enhances YAP/TAZ localization and nuclear translocation in $CD4^+$ T cells. (**a**) Representative immunofluorescence images showing YAP (left) and TAZ (right) localization in $CD4^+$ T cells after LIPUS treatment (1.0 MHz, 20 mW/cm², 2 h/day for 3 days). Nuclei were counterstained with DAPI (blue). Top row: low-magnification overview (100X). Bottom row: higher-magnification views of the regions indicated by the white dashed boxes in the panels above. Scale bars: 200 μm (top row), 100 μm (bottom row). (**b**) Quantification of the relative mean fluorescence intensity (MFI) normalized to the untreated control (Ctrl). Data are presented as mean ± SEM from three independent experiments (n=3; ≥50 cells quantified per group per experiment). Statistical significance was determined by unpaired *t*-test with Welch's correction: *p<0.05, ***p<0.001 vs untreated controls.

suppressed *RORγt* mRNA expression (Figure 3b). Additionally, ELISA confirmed reduced secretion of the Th17-associated cytokines IL-17A and IL-23 following LIPUS treatment (Figure 3c).

While we established LIPUS modulates Treg/Th17 balance, the underlying mechanism remained unclear. Given the established role of YAP and TAZ as core mechanotransducers,[22–24] we investigated whether LIPUS affects YAP/TAZ signaling. Our results demonstrate LIPUS significantly enhances YAP/TAZ protein expression and promotes their nuclear translocation (Figure 4), a prerequisite for transcriptional co-activation. This aligns with prior findings showing LIPUS increases YAP expression, nuclear localization, and reduces YAP phosphorylation[42] and facilitates YAP nuclear translocation in 3T3-L1 cells.[43] We propose two complementary mechanisms for LIPUS-mediated YAP/TAZ activation: 1) Enhanced membrane permeability and metabolism: LIPUS may improve membrane permeability and extracellular enzyme activity,[42] potentially boosting YAP/TAZ expression through increased anabolic activity; 2) Direct mechanotransduction: As a low-intensity mechanical stimulus generating negligible cavitation or thermal effects, LIPUS directly modulates YAP/TAZ expression and activity - consistent with known responses to mechanical cues.[44] These mechanisms are supported by our experimental data: Immunofluorescence confirmed LIPUS-induced YAP/TAZ nuclear accumulation (Figure 4a) and an overall increase in their protein levels confirmed by the relative MFI analysis (Figure 4b).

Furthermore, our data indicate that both YAP and TAZ are involved in regulating the expression of Treg- and Th17-associated markers, and that their functions may be redundant in this context. This finding extends prior reports linking YAP/TAZ signaling to T cell function.[19,20] Specifically, siRNA-mediated knockdown of either YAP or TAZ was

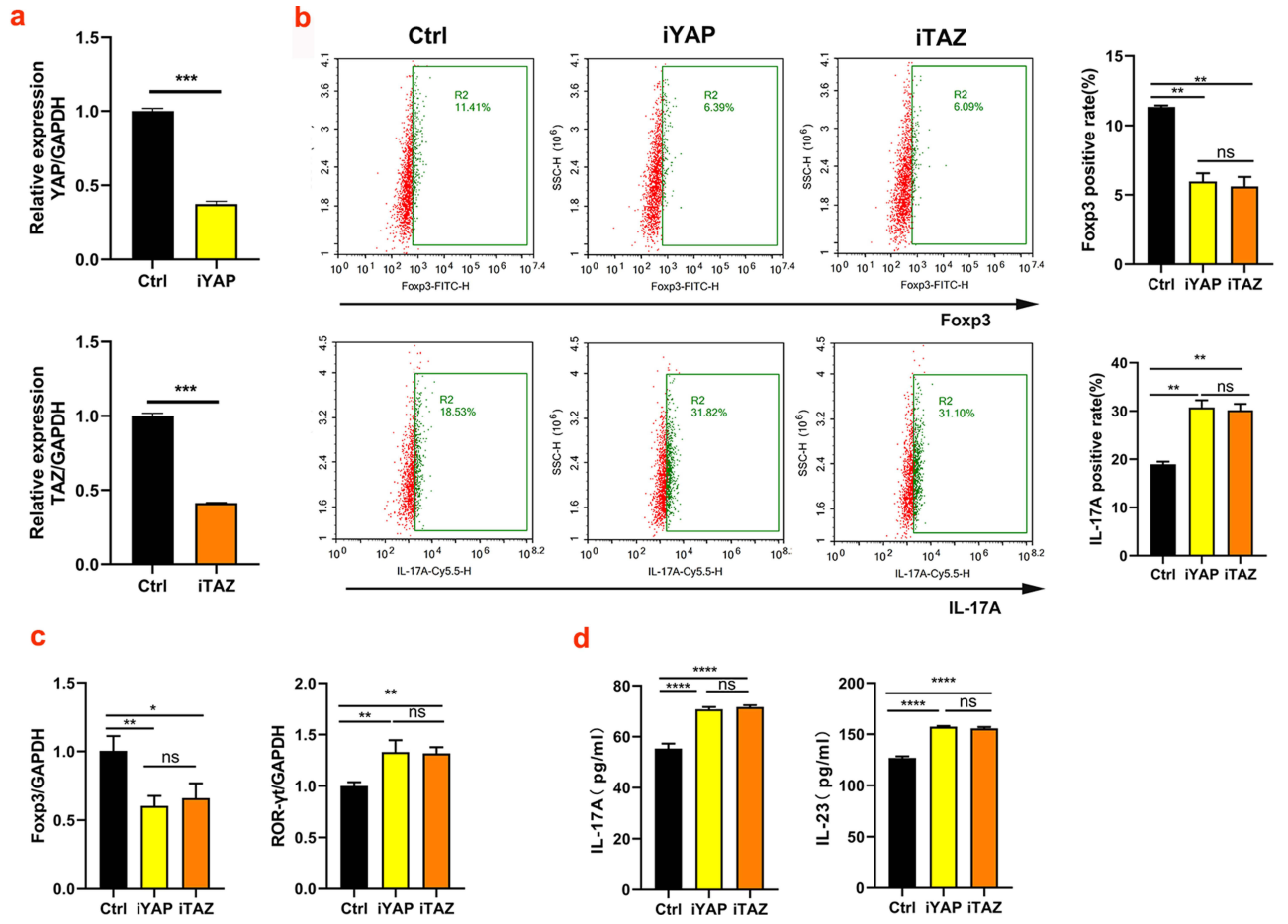

Figure 5 YAP/TAZ knockdown modulates the expression of Treg/Th17-associated markers. (**a**) RT-qPCR analysis confirming the efficiency of YAP and TAZ gene knockdown using target-specific siRNAs ("iYAP" and "iTAZ" groups) compared to a non-targeting scrambled siRNA control ("Ctrl" group). (**b–d**) The impact of YAP/TAZ knockdown on the expression of key functional markers: (**b**) Flow cytometry quantification of Foxp3 and IL-17A protein expression. (**c**) qPCR measurement of *Foxp3* and *RORγt* mRNA levels. (**d**) ELISA quantification of IL-17A and IL-23 cytokine secretion. Data represent mean ± SEM (n=3 biological replicates). Statistical significance was determined by one-way ANOVA with Tukey's post hoc test: *p<0.05, **p<0.01, ***p<0.001, ****p<0.0001 versus the scrambled siRNA control group (Ctrl); ns = not significant.

sufficient to decrease the frequency of Foxp3-positive cells and increase the frequency of IL-17A-positive cells, concurrently elevating the secretion of the Th17-related cytokines IL-17A and IL-23 (Figure 5). The fact that knockdown of either YAP or TAZ alone produced a similar magnitude of effect on the expression of Treg/Th17-associated markers suggests a potential functional redundancy or compensatory mechanism between these two transcriptional coactivators.[45,46] It is possible that the loss of one paralog is partially compensated by the increased activity or expression of the other, a phenomenon well-documented in other systems.[47,48] Furthermore, other Hippo pathway effectors or interaction partners, such as TEAD transcription factors, may also play a role in maintaining the regulatory output upon partial pathway disruption.[49] Future studies employing double-knockout models would be required to definitively test this hypothesis and unravel the precise compensatory networks at play. Our data, which point to redundancy in this context, contrast with reports of distinct roles for TAZ in modulating Foxp3 acetylation and RORγt activity,[39] highlighting the context-dependent functions of these mechanosensors. Crucially, applying LIPUS to YAP/TAZ-knockdown cells significantly mitigated the Treg/Th17 imbalance caused by siRNA (Figure 7a). LIPUS upregulated YAP/TAZ fluorescence signals (Figure 6) and downstream transcriptional activity (Figure 7b and c), confirming their mechanistic involvement.

Key Mechanistic Insights:

1. Suppression of Th17-associated responses: The LIPUS-mediated reduction of IL-17A production and RORγt expression was strictly dependent on YAP/TAZ activity. In both the iYAPL and iTAZL groups, the suppressive effect on Th17-

https://doi.org/10.2147/JIR.S548291

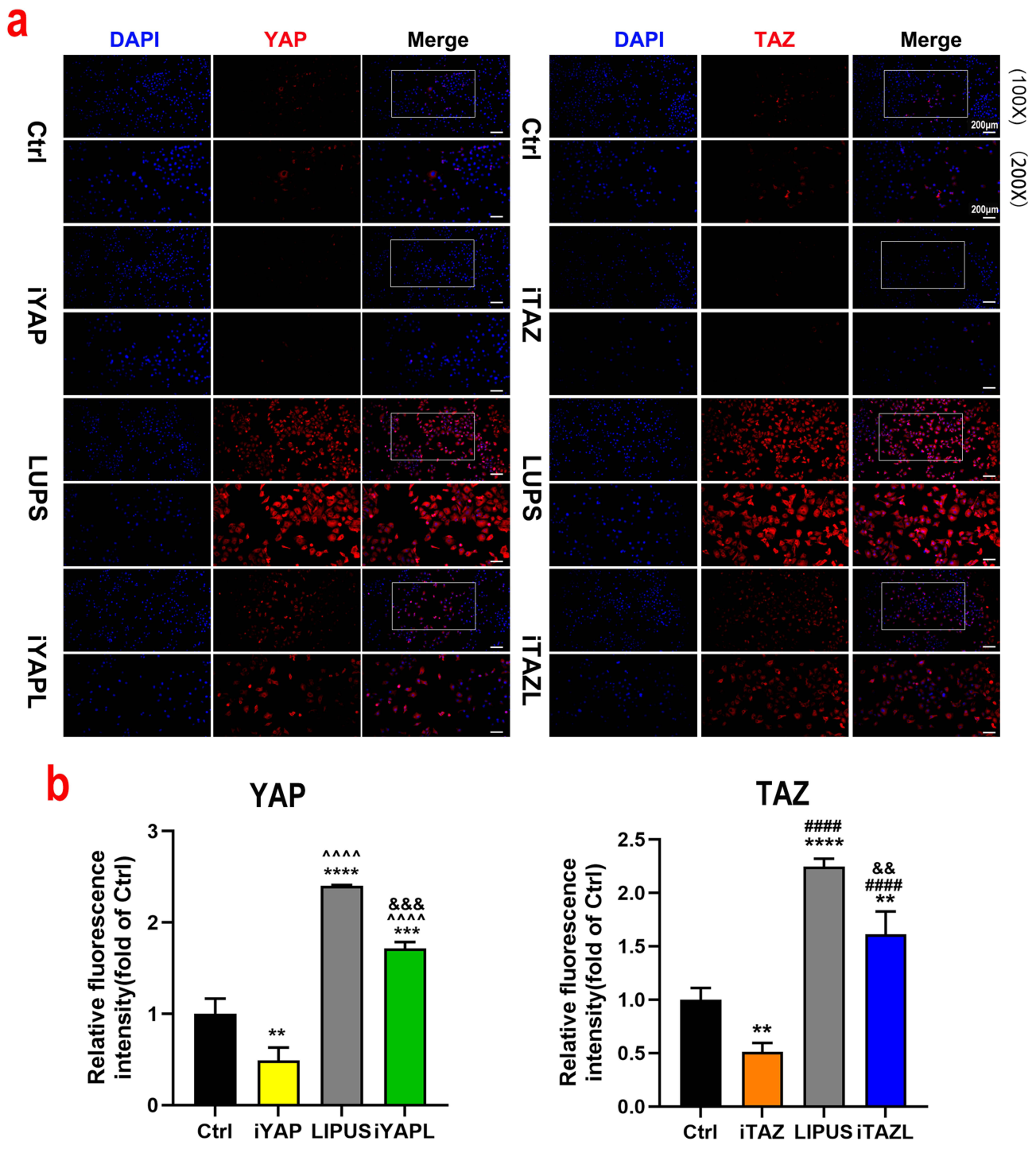

Figure 6 LIPUS mitigating the functional consequences following siRNA-mediated knockdown. of knockdown (**a**) Representative immunofluorescence images of YAP (left) and TAZ (right) in $CD4^+$ T cells under six treatment conditions: untreated control (Ctrl), YAP knockdown (iYAP), TAZ knockdown (iTAZ), LIPUS alone (LIPUS), YAP knockdown + LIPUS (iYAPL), and TAZ knockdown + LIPUS (iTAZL). LIPUS treatment (1.0 MHz, 20 mW/cm², 20% duty cycle, 2 h/day for 3 days) restored the subcellular localization of YAP and TAZ in siRNA-transfected cells. Nuclei were counterstained with DAPI (blue). Top row: low-magnification overview (100X). Bottom row: higher-magnification views of the regions indicated by the white dashed boxes in the panels above. Scale bars: 200 μm (top row), 100 μm (bottom row). (**b**) Quantification of the relative mean fluorescence intensity (MFI) normalized to the untreated control (Ctrl) group. Data are presented as mean ± SEM from three independent experiments (n=3; ≥50 cells quantified per group per experiment). Statistical significance was determined by one-way ANOVA with Tukey's multiple comparisons test: **p<0.01, ***p<0.001, ****p<0.0001 vs Ctrl; ^^^^p<0.0001 vs iYAP; ####p<0.0001 vs iTAZ; &&p<0.01, &&&p<0.001 vs LIPUS; ns=not significant.

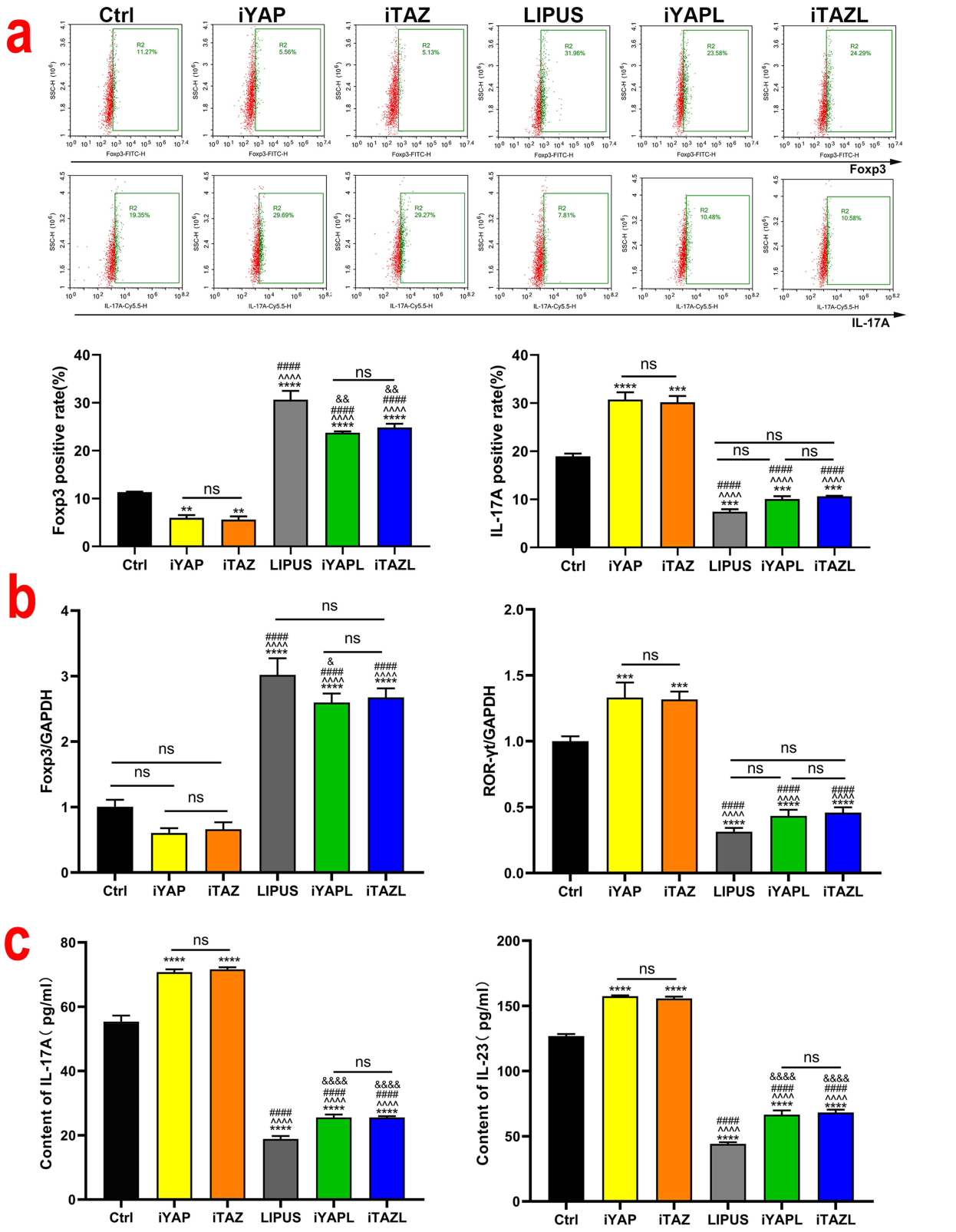

Figure 7 YAP/TAZ signaling is involved in LIPUS-mediated modulation of Treg/Th17-associated markers. $CD4^+$ T cells were divided into six experimental groups: (1) Untreated controls (Ctrl), (2) YAP knockdown (iYAP), (3) TAZ knockdown (iTAZ), (4) LIPUS alone (LIPUS), (5) YAP knockdown + LIPUS (iYAPL), and (6) TAZ knockdown + LIPUS (iTAZL). Cells were treated with LIPUS (1.0 MHz, 20 mW/cm², 20% duty cycle, 2 h/day) for 72 hours following siRNA transfection. (**a**) Representative flow cytometry plots showing Foxp3 and IL-17A expression. Upper: Representative flow plots. Lower: Quantification of the frequencies of $Foxp3^+$ and $IL\text{-}17A^+$ cells. (**b**) qPCR analysis of *Foxp3* and *RORγt* mRNA levels. (**c**) ELISA quantification of IL-17A, IL-23, and IL-10 cytokine secretion. Statistical significance was determined by two-way ANOVA with Tukey's multiple comparisons test: **p<0.01, ***p<0.001, ****p<0.0001 vs Ctrl; ^^^^p<0.0001 vs iYAP; #####p<0.0001 vs iTAZ; &p<0.05, &&p<0.01, &&&&<0.0001 vs LIPUS; ns=not significant.

https://doi.org/10.2147/JIR.S548291

associated markers was substantially mitigated, returning to levels comparable to those observed with LIPUS treatment alone. This recovery of immunomodulatory function confirms the essential role of YAP/TAZ signaling in this process.

2. Promotion of Treg-associated characteristics: While YAP/TAZ signaling appears to be the primary mechanism underlying the LIPUS-induced increase in Foxp3 expression, our data suggest that additional, complementary pathways may contribute to this effect.

In the present study, the use of total $CD4^+$ T cells was primarily chosen to model a scenario in vitro where LIPUS (eg, during a therapeutic application) might directly act on the mixed population of T cells present in the peripheral circulation. This approach is further supported by recent in vivo findings from Fu et al[50] who demonstrated that LIPUS can protect against immune checkpoint inhibitor-related myocarditis in mice by precisely fine-tuning the balance of $CD4^+$ T-cell subpopulations, providing direct evidence for the physiological relevance of LIPUS-mediated modulation of circulating $CD4^+$ T cells. While we acknowledge that this setup cannot strictly distinguish whether the observed effects are due to the differentiation of naïve $CD4^+$ T cells or the modulation of pre-existing effector/memory cell functions and populations, our findings reveal that LIPUS possesses a potent capacity to directly and rapidly modulate the functional state of more mature T cells. This represents a crucial mechanism for immune regulation in its own right. However, we certainly agree that investigating the impact of LIPUS on the differentiation of naïve $CD4^+$ T cells is a fascinating and critical next step, and it is a central part of our planned future work. While our data strongly suggest the involvement of YAP/TAZ, future studies employing functional assays (eg, T cell suppression assays for Treg function) in conjunction with YAP/TAZ modulation are required to formally establish causal relationships and demonstrate functional differentiation. Our findings support a model in which LIPUS activates a mechanotransductive pathway to modulate $CD4^+$ T cell function, promoting a Treg-like immunomodulatory profile while suppressing Th17-associated responses, largely through the activation of YAP/TAZ signaling. While this mechanistic link was rigorously demonstrated in vitro, critical next steps include validating these effects in preclinical models of immune dysregulation to evaluate their physiological relevance and therapeutic potential, elucidating the precise molecular events downstream of YAP/TAZ that drive the observed shifts in functional marker expression, and investigating potential LIPUS effects on other immune cell types within the inflammatory microenvironment, such as dendritic cells and macrophages.

Conclusion

In this study, we demonstrate that low-intensity pulsed ultrasound (LIPUS) modulates the balance between Treg- and Th17-associated immune responses through the YAP/TAZ signaling pathway. LIPUS enhanced YAP/TAZ protein levels, increased the frequency of Foxp3-positive cells, and reduced the population of IL-17A-producing cells. Genetic inhibition of YAP or TAZ expression skewed the profile toward Th17-associated markers, while LIPUS treatment counteracted this effect and restored the balance by activating YAP/TAZ signaling to promote Treg-like immunomodulatory function. Further studies are needed to fully elucidate the precise molecular mechanisms underlying LIPUS-mediated immunomodulation. Our findings reveal a previously unexplored mechano-immunological role of LIPUS and provide a conceptual foundation for its potential application in immune modulation.

Data Sharing Statement

The data used to support the findings of this study are available from the corresponding author upon request.

Ethical Approval

All animal experiments described in this report were approved by the Sichuan University Animal Care and Use Committee. In total, 50 Sprague-Dawley rats were used. The ethics committee number of this experiment is WCHSIRB-D-2020043.

Funding

This work was supported by Key R&D Project of the Science and Technology Department of Sichuan Province, China (Grant No. 2024YFFK0375), and the Exploratory and R&D Project of West China Hospital of Stomatology, Sichuan University (Grant No. LCYJ2023-YY-1).

Disclosure

The authors declare no financial or personal relationships with other people or organizations that can inappropriately influence our work. There is no professional or other personal interest of any nature or kind in any product, service, and/or company that could be construed as influencing the position presented in, or the review of, the manuscript.

References

1. Jin S, Chen H, Li Y. et al. Maresin 1 improves the Treg/Th17 imbalance in rheumatoid arthritis through miR-21. *Ann Rheumatic Dis*. 2018;77(11):1644–1652. doi:10.1136/annrheumdis-2018-213511
2. Loi F, Córdova LA, Pajarinen J, Lin TH, Yao Z, Goodman SB. Inflammation, fracture and bone repair. *Bone*. 2016;86:119–130. doi:10.1016/j.bone.2016.02.020
3. Liu YJ, Tang B, Wang FC, et al. Parthenolide ameliorates colon inflammation through regulating Treg/Th17 balance in a gut microbiota-dependent manner. *Theranostics*. 2020;10(12):5225–5241. doi:10.7150/thno.43716
4. Lee GR. The Balance of Th17 versus Treg Cells in Autoimmunity. *Int J Mol Sci*. 2018;19(3):730. doi:10.3390/ijms19030730
5. Pawlak M, Ho AW, Kuchroo VK. Cytokines and transcription factors in the differentiation of CD4(+) T helper cell subsets and induction of tissue inflammation and autoimmunity. *Curr Opin Immunol*. 2020;67:57–67. doi:10.1016/j.coi.2020.09.001
6. Whiteside TL. FOXP3+ Treg as a therapeutic target for promoting anti-tumor immunity. *Expert Opinion on Therapeutic Targets*. 2018;22(4):353–363. doi:10.1080/14728222.2018.1451514
7. Gagliani N, Amezcua Vesely MC, Iseppon A, et al. Th17 cells transdifferentiate into regulatory T cells during resolution of inflammation. *Nature*. 2015;523(7559):221–225. doi:10.1038/nature14452
8. Srivastava RK, Dar HY, Mishra PK. Immunoporosis: immunology of Osteoporosis-Role of T Cells. *Front Immunol*. 2018;9:657. doi:10.3389/fimmu.2018.00657
9. Miossec P, Kolls JK. Targeting IL-17 and TH17 cells in chronic inflammation. *Nat Rev Drug Discov*. 2012;11(10):763–776. doi:10.1038/nrd3794
10. Razawy W, van Driel M, Lubberts E. The role of IL-23 receptor signaling in inflammation-mediated erosive autoimmune arthritis and bone remodeling. *Eur J Immunol*. 2018;48(2):220–229. doi:10.1002/eji.201646787
11. Knochelmann HM, Dwyer CJ, Bailey SR, et al. When worlds collide: th17 and Treg cells in cancer and autoimmunity. *Cell Mol Immunol*. 2018;15(5):458–469. doi:10.1038/s41423-018-0004-4
12. Huber S, Gagliani N, Flavell RA. Life, death, and miracles: th17 cells in the intestine. *Eur J Immunol*. 2012;42(9):2238–2245. doi:10.1002/eji.201242619
13. Heink S, Yogev N, Garbers C, et al. Trans-presentation of IL-6 by dendritic cells is required for the priming of pathogenic T(H)17 cells. *Nat Immunol*. 2017;18(1):74–85. doi:10.1038/ni.3632
14. Mangan PR, Harrington LE, O'Quinn DB, et al. Transforming growth factor-beta induces development of the T(H)17 lineage. *Nature*. 2006;441(7090):231–234. doi:10.1038/nature04754
15. Ohkura N, Kitagawa Y, Sakaguchi S. Development and maintenance of regulatory T cells. *Immunity*. 2013;38(3):414–423. doi:10.1016/j.immuni.2013.03.002
16. Li MO, Rudensky AY. T cell receptor signalling in the control of regulatory T cell differentiation and function. *Nat Rev Immunol*. 2016;16(4):220–233. doi:10.1038/nri.2016.26
17. Coombes JL, Siddiqui KR, Arancibia-Cárcamo CV, et al. A functionally specialized population of mucosal CD103+ DCs induces Foxp3+ regulatory T cells via a TGF-beta and retinoic acid-dependent mechanism. *J Exp Med*. 2007;204(8):1757–1764. doi:10.1084/jem.20070590
18. Rodríguez-Jiménez P, Chicharro P, Llamas-Velasco M, et al. Thrombospondin-1/CD47 Interaction Regulates Th17 and Treg Differentiation in Psoriasis. *Front Immunol*. 2019;10:1268. doi:10.3389/fimmu.2019.01268
19. Ni X, Tao J, Barbi J, et al. YAP Is Essential for Treg-Mediated Suppression of Antitumor Immunity. *Cancer Discov*. 2018;8(8):1026–1043. doi:10.1158/2159-8290.CD-17-1124
20. Ramjee V, Li D, Manderfield LJ, et al. Epicardial YAP/TAZ orchestrate an immunosuppressive response following myocardial infarction. *J Clin Invest*. 2017;127(3):899–911. doi:10.1172/jci88759
21. Yue Y, Yang X, Zhang L, et al. Low-intensity pulsed ultrasound upregulates pro-myelination indicators of Schwann cells enhanced by co-culture with adipose-derived stem cells. *Cell Prolif*. 2016;49(6):720–728. doi:10.1111/cpr.12298
22. Panciera T, Azzolin L, Cordenonsi M, Piccolo S. Mechanobiology of YAP and TAZ in physiology and disease. *Nat Rev Mol Cell Biol*. 2017;18(12):758–770. doi:10.1038/nrm.2017.87
23. Dupont S, Morsut L, Aragona M, et al. Role of YAP/TAZ in mechanotransduction. *Nature*. 2011;474(7350):179–183. doi:10.1038/nature10137
24. Totaro A, Panciera T, Piccolo S. YAP/TAZ upstream signals and downstream responses. *Nat Cell Biol*. 2018;20(8):888–899. doi:10.1038/s41556-018-0142-z
25. Xu XM, Xu TM, Wei YB, et al. Low-Intensity Pulsed Ultrasound Treatment Accelerates Angiogenesis by Activating YAP/TAZ in Human Umbilical Vein Endothelial Cells. *Ultrasound Med Biol*. 2018;44(12):2655–2661. doi:10.1016/j.ultrasmedbio.2018.07.007
26. Jiang X, Savchenko O, Li Y, et al. A Review of Low-Intensity Pulsed Ultrasound for Therapeutic Applications. *IEEE Transac Bio-Medl Eng*. 2019;66(10):2704–2718. doi:10.1109/tbme.2018.2889669
27. Sang F, Xu J, Chen Z, Liu Q, Jiang W. Low-Intensity Pulsed Ultrasound Alleviates Osteoarthritis Condition Through Focal Adhesion Kinase-Mediated Chondrocyte Proliferation and Differentiation. *Cartilage*. 2020;2020:1947603520912322. doi:10.1177/1947603520912322
28. Elvey MH, Miller R, Khor KS, Protopapa E, Horwitz MD, Hunter AR. The use of low-intensity pulsed ultrasound in hand and wrist nonunions. *J Plastic Surg Hand Surg*. 2020;54(2):101–106. doi:10.1080/2000656x.2019.1693393
29. Wu Y, Gao Q, Zhu S, et al. Low-intensity pulsed ultrasound regulates proliferation and differentiation of neural stem cells through notch signaling pathway. *Biochem Biophys Res Commun*. 2020;526(3):793–798. doi:10.1016/j.bbrc.2020.03.142
30. Shiraishi R, Masaki C, Toshinaga A, et al. The effects of low-intensity pulsed ultrasound exposure on gingival cells. *Journal of Periodontology*. 2011;82(10):1498–1503. doi:10.1902/jop.2011.100627

31. Yue Y, Yang X, Wei X, et al. Osteogenic differentiation of adipose-derived stem cells prompted by low-intensity pulsed ultrasound. *Cell Proliferation*. 2013;46(3):320–327. doi:10.1111/cpr.12035
32. Zhu J, Yamane H, Paul WE. Differentiation of effector CD4 T cell populations (*). *Ann Rev Immunol*. 2010;28(1):445–489. doi:10.1146/annurev-immunol-030409-101212
33. Zhang Y, Liu Z, Tian M, et al. The altered PD-1/PD-L1 pathway delivers the 'one-two punch' effects to promote the Treg/Th17 imbalance in pre-eclampsia. *Cell Mol Immunol*. 2018;15(7):710–723. doi:10.1038/cmi.2017.70
34. Ding JW, Zheng XX, Zhou T, Tong XH, Luo CY, Wang XA. HMGB1Modulates the Treg/Th17 Ratio in Atherosclerotic Patients. *J Atherosclerosi Thrombosis*. 2016;23(6):737–745. doi:10.5551/jat.31088
35. Liu Y, Yan W, Yuan W, et al. Treg/Th17 imbalance is associated with poor autoimmune hepatitis prognosis. *Clin Immunol*. 2019;198:79–88. doi:10.1016/j.clim.2018.11.003
36. Rajendran M, Looney S, Singh N, et al. Systemic Antibiotic Therapy Reduces Circulating Inflammatory Dendritic Cells and Treg-Th17 Plasticity in Periodontitis. *J Immunol*. 2019;202(9):2690–2699. doi:10.4049/jimmunol.1900046
37. Wang D, Huang S, Yuan X, et al. The regulation of the Treg/Th17 balance by mesenchymal stem cells in human systemic lupus erythematosus. *Cell Mol Immunol*. 2017;14(5):423–431. doi:10.1038/cmi.2015.89
38. Cui H, Cai Y, Wang L, et al. Berberine Regulates Treg/Th17 Balance to Treat Ulcerative Colitis Through Modulating the Gut Microbiota in the Colon. *Front Pharmacol*. 2018;9:571. doi:10.3389/fphar.2018.00571
39. Geng J, Yu S, Zhao H, et al. The transcriptional coactivator TAZ regulates reciprocal differentiation of TH17 cells and Treg cells. *Nat Immunol*. 2017;18(7):800–812. doi:10.1038/ni.3748
40. Poolman RW, Agoritsas T, Siemieniuk RA, et al. Low intensity pulsed ultrasound (LIPUS) for bone healing: a clinical practice guideline. *BMJ*. 2017;356:j576. doi:10.1136/bmj.j576
41. Shirakata Y, Imafuji T, Sena K, Shinohara Y, Nakamura T, Noguchi K. Periodontal tissue regeneration after low-intensity pulsed ultrasound stimulation with or without intra-marrow perforation in two-wall intra-bony defects-A pilot study in dogs. *J Clinical Periodontol*. 2020;47(1):54–63. doi:10.1111/jcpe.13197
42. Zhou JX, Liu YJ, Chen X, et al. Low-Intensity Pulsed Ultrasound Protects Retinal Ganglion Cell From Optic Nerve Injury Induced Apoptosis via Yes Associated Protein. *Front Cell Neurosci*. 2018;12:160. doi:10.3389/fncel.2018.00160
43. Nishida T, Nagao Y, Hashitani S, Yamanaka N, Takigawa M, Kubota S. Suppression of adipocyte differentiation by low-intensity pulsed ultrasound via inhibition of insulin signaling and promotion of CCN family protein 2. *J Cell Biochem*. 2020;121(12):4724–4740. doi:10.1002/jcb.29680
44. Boopathy GTK, Hong W. Role of Hippo Pathway-YAP/TAZ Signaling in Angiogenesis. *Front Cell Develop Biol*. 2019;7:49. doi:10.3389/fcell.2019.00049
45. Yang W, Zhang M, Zhang TX, et al. YAP/TAZ mediates resistance to KRAS inhibitors through inhibiting proapoptosis and activating the SLC7A5/mTOR axis. *JCI Insight*. 2024;9(24). doi:10.1172/jci.insight.178535
46. Chuang LSH, Ito Y. The Multiple Interactions of RUNX with the Hippo-YAP Pathway. *Cells*. 2021;10(11):2925. doi:10.3390/cells10112925
47. Li L, Tang J, Cao B, et al. GPR137 inactivates Hippo signaling to promote gastric cancer cell malignancy. *Biology Direct*. 2024;19(1):3. doi:10.1186/s13062-023-00449-8
48. Bae JS, Kim SM, Jeon Y, et al. Loss of Mob1a/b impairs the differentiation of mouse embryonic stem cells into the three germ layer lineages. *Exop Mol Med*. 2019;51(11):1–12. doi:10.1038/s12276-019-0342-z
49. Masliantsev K, Karayan-Tapon L, Guichet PO. Hippo Signaling Pathway in Gliomas. *Cells*. 2021;10(1):184. doi:10.3390/cells10010184
50. Fu S, Guo Z, Xu X, et al. Protective effect of low-intensity pulsed ultrasound on immune checkpoint inhibitor-related myocarditis via fine-tuning CD4(+) T-cell differentiation. *CII*. 2024;73(1):15. doi:10.1007/s00262-023-03590-5